SCIENTIFIC REPORTS

OPEN

Turn-on Luminescent Probe for Hydrogen Peroxide Sensing and Imaging in Living Cells based on an Iridium(III) Complex–Silver Nanoparticle Platform

Received: 20 June 2017
Accepted: 25 July 2017
Published online: 21 August 2017

Jinshui Liu[1,2], Zhen-Zhen Dong[2], Chao Yang[3], Guodong Li[3], Chun Wu[2], Fu-Wa Lee[4], Chung-Hang Leung[3] & Dik-Lung Ma[2]

A sensitive turn-on luminescent sensor for H_2O_2 based on the silver nanoparticle (AgNP)-mediated quenching of an luminescent Ir(III) complex (Ir-1) has been designed. In the absence of H_2O_2, the luminescence intensity of Ir-1 can be quenched by AgNPs via non-radiative energy transfer. However, H_2O_2 can oxidize AgNPs to soluble Ag^+ cations, which restores the luminescence of Ir-1. The sensing platform displayed a sensitive response to H_2O_2 in the range of 0—17 μM, with a detection limit of 0.3 μM. Importantly, the probe was successfully applied to monitor intracellular H_2O_2 in living cells, and it also showed high selectivity for H_2O_2 over other interfering substances.

H_2O_2 is widely used in industry and households for rinsing, bleaching and disinfection. For example, in the food industry, H_2O_2 is used to replace chlorine-containing bleaching and sterilizing agents[1]. It also plays an important role in many biological processes and enzymatic reactions, particularly those related to intracellular oxidative stress[2]. In fact, escalated levels of H_2O_2 can cause irreversible cellular damage through the oxidation of biomolecules, leading to cell death[3]. Moreover, oxidative damage to cellular proteins, nucleic acids, and lipid molecules are associated with aging and age-related disorder ranging from neurodegeneration to diabetes[3,4]. Therefore, a rapid and reliable detection of H_2O_2 is important in pharmaceutical, clinical, and food industries.

Multiple methods such as spectrophotometry[5,6], chemiluminescence[7] and electrocatalysis[8] have been developed for the detection of H_2O_2. Specifically, biosensors have been developed on the basis of electrocatalysis of immobilized enzymes arising from H_2O_2 reduction[9]. However, the enzyme-based biosensors are limited by sensitivity to environmental conditions, high cost, short shelf-life and complicated immobilization procedures[10–12]. Meanwhile, fluorescent strategies have lots of advantages, particularly rapid response, high sensitivity, and simple manipulation[13,14]. Various fluorescence probes such as organic molecules[15], carbon dots[16,17], metal nanoclusters[18], and nanoparticles[19–21], have good performance on the determination of H_2O_2. However, there are still some drawbacks for these reported probes, including poor sensitivity and selectivity, low stability in biological environment, or complicated operation[17,18,22]. Fluorescence turn-on sensors are generally more desirable than fluorescence quenching sensors as the former is less susceptible to false positive signals[23,24].

Luminescent Ir(III) complexes have been employed to detect a variety of analytes[25–27]. Compared with organic molecules, Ir(III) complexes generally exhibit large Stokes shifts, ease in synthesis and long-lived luminescence which could be distinguished from fluorescence noise in biological matrices[26,27]. Meanwhile, silver nanoparticles (AgNPs) form a promising nanomaterial that has been developed in many applications because of their remarkable properties, such as high extinction coefficient and surface plasmon resonance absorption[28–30]. It has been reported that AgNPs can be oxidized by traces of H_2O_2, to form Ag^+[31]. In addition, AgNPs can function as

[1]College of Chemistry and Materials Science, Anhui Normal University, Wuhu, China. [2]Department of Chemistry, Hong Kong Baptist University, Kowloon Tong, Hong Kong, China. [3]State Key Laboratory of Quality Research in Chinese Medicine, Institute of Chinese Medical Sciences, University of Macau, Macao, China. [4]College of International Education, School of Continuing Education, Hong Kong Baptist University, Shek Mun, Hong Kong, China. Jinshui Liu and Zhen-Zhen Dong contributed equally to this work. Correspondence and requests for materials should be addressed to D.-L.M. (email: edmondma@hkbu.edu.hk)

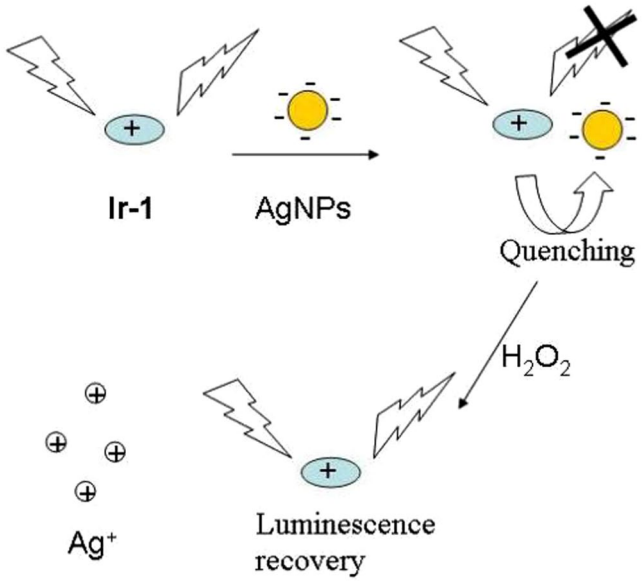

Figure 1. Illustration of the design rationale for the detection of H_2O_2 using a luminescence sensor based on **Ir-1**–AgNPs system.

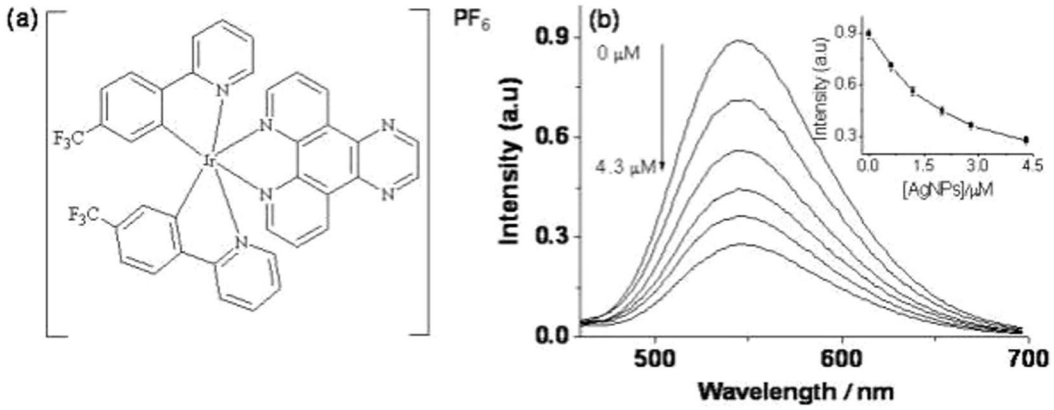

Figure 2. (**a**) Chemical structure of **Ir-1**. (**b**) Luminescence emission spectra 0.3 μM **Ir-1** in Tris-HNO_3 buffer solution (pH 7.0) containing different concentrations of AgNPs. The inset is the luminescence intensity at 545 nm plotted against the AgNPs concentration.

excellent quenchers for fluorescent materials, such as organic dyes and quantum dots (QDs)[32–35]. However, as far as we know, the application of the Ir(III) complexes combined with AgNPs has not yet been reported in the literature for H_2O_2 sensing. Consequently, taking advantages of the Ir(III) complex (**Ir-1**, $[Ir(tfppy)_2(pyphen)]^+$, where tfppy = 2-[4-(trifluoromethyl)phenyl]pyridine, pyphen = pyrazino[2,3-*f*][1,10]phenanthroline) and AgNPs, we designed a novel turn-on luminescent probe for rapid and sensitive detection of intracellular H_2O_2.

The sensing mechanism of the **Ir-1**–AgNP probe for H_2O_2 is illustrated in Fig. 1. In the initial system, the luminescence of **Ir-1** was significantly quenched by AgNPs. However, this AgNPs-induced quenching effect can be reversed by H_2O_2 due to oxidation of AgNPs to Ag^+. To our knowledge, the **Ir-1**–AgNP is the first application of the combination of Ir(III) complexes and AgNPs for H_2O_2 sensing in both aqueous solutions and living cells.

Results and Discussion

Sensing Mechanism. **Ir-1**, carrying tfppy as its C^N ligand and pyphen as its N^N ligand (Fig. 2a), was characterized by ^{1}H-NMR, ^{13}C-NMR and HRMS (Figs S1–S3 and Table S1). **Ir-1** emits strong luminescence at 545 nm under the excitation of 295 nm in aqueous buffer solution. As expected, the luminescence of **Ir-1** decreased gradually with increasing amounts of AgNPs in solution (Fig. 2b). This is because the positively charged **Ir-1** could be adsorbed on the surface of the citrate-stabilized AgNPs through electrostatic interactions, which efficiently quenched the luminescence of **Ir-1**. However, the luminescence could be recovered in the presence of H_2O_2 attributed to oxidation of AgNPs into soluble Ag^+ by H_2O_2. In order to study the kinetic behavior between the **Ir-1**–AgNP system and H_2O_2, the luminescence change was monitored as a function of time. As shown in

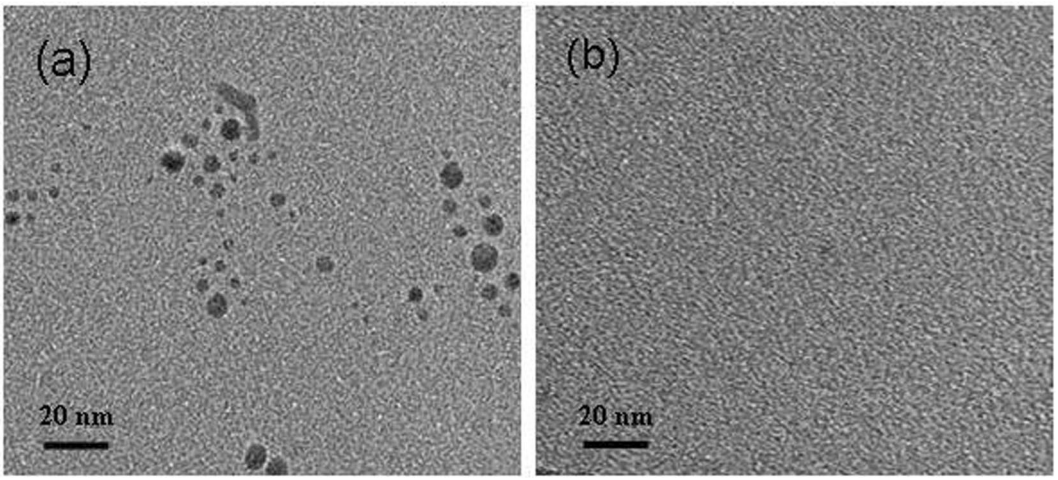

Figure 3. Transmission electron microscopy images of (**a**) AgNPs and (**b**) AgNPs in the presence of H_2O_2.

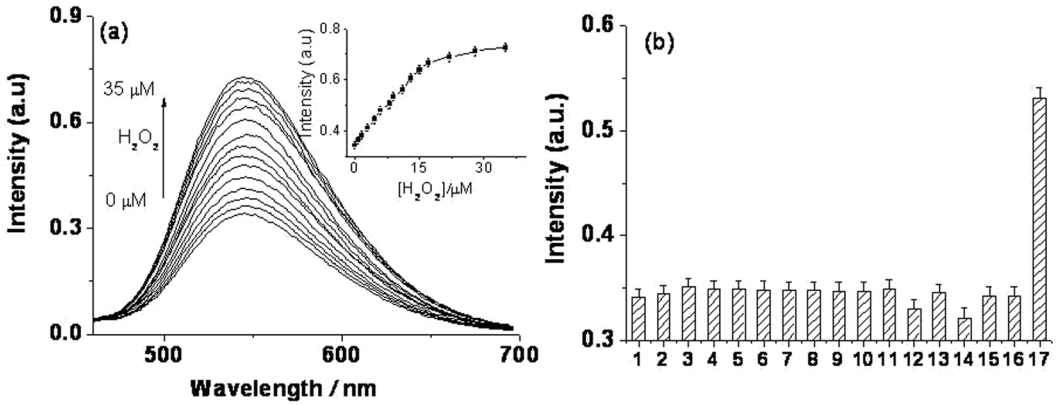

Figure 4. (**a**) Luminescence emission spectra of 1 μM **Ir-1** in Tris-HNO_3 buffer solution (pH 7.0) containing 2.8 μM AgNPs and different concentrations of H_2O_2 (0 μM to 35 μM). The inset is the luminescence intensity plotted against the H_2O_2 concentration. (**b**) Luminescence intensity of the **Ir-1**-AgNP system (0.3 μM **Ir-1** and 2.8 μM AgNPs in Tris-HNO_3 at pH 7.0) in the presence of interfering species (HSA and BSA 50 μg/L, other interfering species 50 μM) or H_2O_2 (9 μM) (from 1 to 17: blank, threonine, serine, glycine, ascorbic acid, HSA, BSA, Zn^{2+}, Co^{2+}, Ni^{2+}, Cd^{2+}, Fe^{3+}, Mg^{2+}, Cu^{2+}, K^+, Na^+, and H_2O_2).

Fig. S4, the luminescence intensity of the **Ir-1**–AgNP system increased with time and reached the plateau after 10 min, indicating that the reaction between AgNPs and H_2O_2 at ambient temperature is rapid. In the absence of AgNPs, H_2O_2 showed no apparent effect on the luminescence of **Ir-1** (Fig. S5). Therefore, the increase in the luminescence of the system should arise primarily from the decomposition of AgNPs by H_2O_2, which restores the emission of **Ir-1**.

The mechanism involved in the luminescence quenching and recovery process was also demonstrated by transmission electron microscopy (TEM) imaging. In the absence of the **Ir-1**, the AgNPs were well-dispersed (Fig. 3a). However, after the addition of **Ir-1**, slight aggregation of AgNPs was observed, suggesting that **Ir-1** and AgNPs interacted on the surface of AgNPs (Fig. S6b). The identity of the **Ir-1**–AgNP complex was further confirmed by energy dispersive X-ray spectroscopy (EDX), which showed strong elemental signals for both Ir and Ag (Fig. S6c). Strikingly, after treatment of AgNPs with H_2O_2, no AgNPs could be observed in the TEM images (Fig. 3b). This suggests that the AgNPs were decomposed and transformed to Ag^+, which is consistent with previously reported[36–38]. The UV–vis absorbance spectra of AgNPs in the absence and presence of H_2O_2 are shown in Fig. S7. AgNPs alone showed a strong characteristic surface plasmon resonance peak at around 390 nm[39]. However, the absorption band of AgNPs gradually decreased upon increasing concentration of H_2O_2. These phenomena were ascribed to the oxidation of AgNPs to Ag^+ by H_2O_2, leading the decomposition of the AgNPs.

Sensitivity. To explore the applicability of the proposed luminescence sensor for H_2O_2 detection, we studied the luminescence response of the **Ir-1**–AgNP system toward varying concentrations of H_2O_2. The luminescence intensity of the system was gradually restored with increasing concentration of H_2O_2 (Fig. 4a). Meanwhile, a good linear relationship over the range from 0 to 17 μmol L^{-1} with a correlation coefficient of 0.998 was obtained (Fig. S8). The limit of detection (LOD) was calculated to 0.3 μM according to the signal-to-noise method

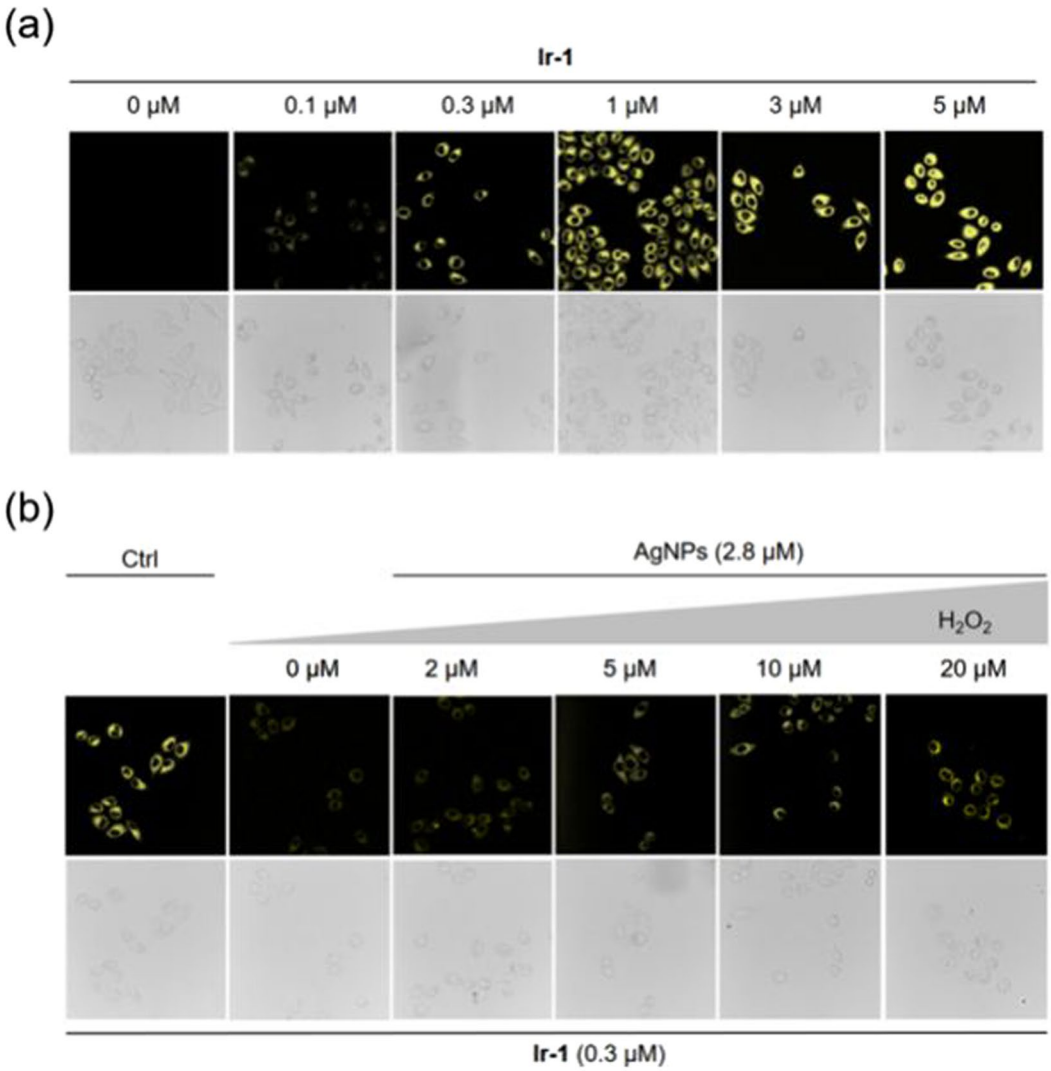

Figure 5. Confocal luminescence microscopy imaging of HeLa cells. (**a**) HeLa cells were incubated with the indicated concentration of **Ir-1** for 1 h. (**b**) HeLa cells were pretreated with **Ir-1** (0.3 μM) and AgNPs (2.8 μM) for 1 h before incubation with different concentration of H_2O_2. The upper row is luminescence imaging, and the lower row is bright field imaging. Excitation wavelength = 405 nm.

(S/N = 3). The sensitivity of this method is comparable to other reported methods for H_2O_2 detection as summarized in Table S2[4,10–16,20,36,40–44].

Selectivity. To assess the selectivity of **Ir-1**–AgNPs system for H_2O_2, the influences of metal ions and amino acids were studied. As shown in Fig. 4b, nearly no luminescence changes could be observed with the other substances (Fig. 4b), which demonstrates that the **Ir-1**–AgNP system is highly selective for H_2O_2 over other non-target substances.

Cell imaging. Given the promising capability of **Ir-1** for sensing H_2O_2 in aqueous solution, we then investigated the ability of **Ir-1** for monitoring H_2O_2 in living human cells. **Ir-1** showed cytotoxicity against HeLa (human cervical cancer) cells with an IC_{50} value of 5.12 μM (Fig. S9).

In the cell imaging study, the luminescence intensity of HeLa cells was enhanced with increasing concentration of **Ir-1** (Fig. 5a), showing that **Ir-1** could effectively penetrate into cells. A concentration of 0.3 μM of **Ir-1** was chosen for subsequent cell experiments as this concentration was over 10-fold lower than the IC_{50} value for cytotoxicity, while it still gave a good luminescence signal.

Next, HeLa cells were pretreated with **Ir-1** (0.3 μM) for 1 h before incubation with different concentration of AgNPs. The luminescence intensity of HeLa cells was remarkably reduced with increasing concentration of AgNPs (Fig. S10), which was attributed to AgNPs-mediated quenching of an luminescent **Ir-1** as described previously. However, when H_2O_2 was added into the growth medium for another 1 h, the luminescence of HeLa cells was recovered in a dose-dependent manner (Fig. 5b). Collectively, these results suggest that **Ir-1**–AgNP can be developed for the monitoring of H_2O_2 levels in living cells.

Conclusion

Consequently, we have proposed a turn-on luminescence assay for H_2O_2 detection employing the **Ir-1**–AgNP system. In this nano-composite system, **Ir-1** functioned as a luminescence reporter, while AgNPs were employed both as a luminescence quencher and as a recognition unit for H_2O_2. Based on the luminescence recovery of the **Ir-1**–AgNP system triggered by H_2O_2, this nanoprobe was successfully applied to detect H_2O_2 at the intracellular level in living cells. In addition, the **Ir-1**–AgNP probe possesses some superior properties, including label-free, good sensitivity and selectivity, low cost, easy manipulation, low cytotoxicity, and turn-on luminescent response. To our knowledge, the probe is the first combination of Ir(III) and AgNPs applied for the detection of H_2O_2 in living cells reported in the literature.

Materials and Methods

Chemicals and materials. Iridium chloride hydrate ($IrCl_3{\cdot}xH_2O$) was purchased from Precious Metals Online (Australia). Other reagents were purchased from Sigma Aldrich (St. Louis, MO) and used as received. All of the reagents were of analytical grade and were used as received without further purification. All solutions were prepared in Milli-Q water under ambient conditions. HeLa cell lines were obtained from ATCC (Manassas, VA, USA). Dulbecco's Modified Eagle's medium, fetal bovine serum, penicillin and streptomycin were obtained from Sigma-Aldrich Co. LLC (St. Louis, MO, USA).

Synthesis of AgNPs. AgNPs were fabricated according to reported methods with slight modifications[28,45]. In a typical procedure, 0.08 mL $AgNO_3$ (0.1 M) and 0.1 mL trisodium citrate (0.1 M) were mixed into 100 mL pure water and stirred under the condition of ice bath. Then, freshly prepared $NaBH_4$ solution was added dropwise into the mixture until it turned yellow. The resulting yellow solution was stirred for another 30 min to form AgNPs quantitatively, which was stored at 4 °C for subsequent use. The diameter of AgNPs prepared was measured to be 8–9 nm by transmission electron microscopy (TEM).

Synthesis of Ir-1. **Ir-1** was synthesized based on a reported literature method[46–49]. $[Ir_2(tfppy)_4Cl_2]$ (0.2 mmol) and pyppy (0.42 mmol) in a mixed solvent of DCM:methanol (1:1.2 (v/v), 36 mL) was refluxed overnight. The reaction mixture was allowed to cool to ambient temperature, and unreacted cyclometallated dimer was removed by filtration. Excess ammonium hexafluorophosphate was then added into the filtrate, and the resulting mixture was stirred for another 30 min. Afterwards, the solution was evaporated under reduced pressure until precipitation was initiated. The precipitate was filtered, and washed by several portions of water and diethyl ether. The crude product was then recrystallized by the acetonitrile/diethyl ether vapor diffusion to obtain the desired compound, which was characterized by ^{1}H-NMR,^{13}C-NMR, high resolution mass spectrometry (HRMS) and elemental analysis.

Luminescence response of Ir-1 towards AgNPs. **Ir-1** (0.3 μM) was added to varying concentrations of AgNPs in Tris-HNO_3 buffer (5 mM Tris-HNO_3, pH 7.0), then their emission intensity were measured.

Detection of H_2O_2. A series of sample solutions of same composition was prepared by mixing **Ir-1** (0.3 μM) with AgNPs (2.8 μM) in Tris-HNO_3 buffer (5 mM Tris-HNO_3, pH 7.0). Upon individual addition of varying concentrations of stock H_2O_2 solution, the sample solutions were incubated for 10 min at room temperature. Emission spectra were collected in the range of 450–700 nm at the excitation wavelength of 295 nm.

Cell imaging. HeLa cells were pretreated with **Ir-1** (0.3 μM) for 1 h at 37 °C, then AgNPs of different concentrations (0 μM, 0.1 μM, 0.3 μM, 1 μM, 3 μM and 5 μM) was added before further incubation for 1 h. After washing with PBS three times, the luminescence intensity of HeLa cells was imaged by a Leica SP8 laser scanning confocal microscope upon excitation at 405 nm.

For H_2O_2 detection, the experiment was performed as above except that after incubation in the presence of AgNPs (2.8 μM), cells were further treated with H_2O_2 ranging from 0 to 20 μM for 1 h. After washing with PBS three times, the luminescence intensity of HeLa cells was then imaged as above.

Statistics analysis. One-way analysis of variance (ANOVA) followed by the Dunnett's method for multiple comparisons by using GraphPad Prism 6.0 was used to analyse the data.

References

1. Liao, Y.-X., Li, K., Wu, M.-Y., Wu, T. & Yu, X.-Q. A selenium-contained aggregation-induced "turn-on" fluorescent probe for hydrogen peroxide. *Organic & biomolecular chemistry* **12**, 3004–3008 (2014).
2. Tian, J. *et al*. Preparation of Ag nanoparticle-decorated poly (m-phenylenediamine) microparticles and their application for hydrogen peroxide detection. *Analyst* **136**, 1806–1809 (2011).
3. Wang, P., Wang, K., Chen, D., Mao, Y. & Gu, Y. A novel colorimetric and near-infrared fluorescent probe for hydrogen peroxide imaging *in vitro* and *in vivo*. *RSC Advances* **5**, 85957–85963 (2015).
4. Peng, R. *et al*. A novel SERS nanoprobe for the ratiometric imaging of hydrogen peroxide in living cells. *Chemical Communications* **52**, 8553–8556 (2016).
5. Wang, F., Liu, X., Lu, C.-H. & Willner, I. Cysteine-mediated aggregation of Au nanoparticles: the development of a H2O2 sensor and oxidase-based biosensors. *ACS nano* **7**, 7278–7286 (2013).
6. Dalui, A. *et al*. Insight into the mechanism revealing the peroxidase mimetic catalytic activity of quaternary CuZnFeS nanocrystals: colorimetric biosensing of hydrogen peroxide and glucose. *Nanoscale* **7**, 9062–9074 (2015).
7. Lee, Y.-D. *et al*. Dye/peroxalate aggregated nanoparticles with enhanced and tunable chemiluminescence for biomedical imaging of hydrogen peroxide. *ACS nano* **6**, 6759–6766 (2012).
8. Su, S. *et al*. Facile Synthesis of a MoS2–Prussian Blue Nanocube Nanohybrid-Based Electrochemical Sensing Platform for Hydrogen Peroxide and Carcinoembryonic Antigen Detection. *ACS Applied Materials & Interfaces* **9**, 12773–12781 (2017).
9. Zhao, B. *et al*. Silver microspheres for application as hydrogen peroxide sensor. *Electrochemistry Communications* **11**, 1707–1710 (2009).

10. Li, Z., Zheng, X. & Zheng, J. A non-enzymatic sensor based on Au@Ag nanoparticles with good stability for sensitive detection of H_2O_2. *New Journal of Chemistry* **40**, 2115–2120 (2016).
11. Wen, T., Qu, F., Li, N. B. & Luo, H. Q. Polyethyleneimine-capped silver nanoclusters as a fluorescence probe for sensitive detection of hydrogen peroxide and glucose. *Analytica chimica acta* **749**, 56–62 (2012).
12. Yan, Y. *et al*. Hydrothermally driven three-dimensional evolution of mesoporous hierarchical europium oxide hydrangea microspheres for non-enzymatic sensors of hydrogen peroxide detection. *Environmental Science: Nano* **3**, 701–706 (2016).
13. Ren, M. *et al*. A Single fluorescent probe for Dual-imaging Viscosity and H_2O_2 in Mitochondria with Different Fluorescence Signals in Living Cells. *Analytical Chemistry* **89**, 552–555 (2016).
14. Wu, G., Zeng, F., Yu, C., Wu, S. & Li, W. A ratiometric fluorescent nanoprobe for H_2O_2 sensing and *in vivo* detection of drug-induced oxidative damage to the digestive system. *Journal of Materials Chemistry B* **2**, 8528–8537 (2014).
15. Weinstain, R., Savariar, E. N., Felsen, C. N. & Tsien, R. Y. *In vivo* targeting of hydrogen peroxide by activatable cell-penetrating peptides. *Journal of the American Chemical Society* **136**, 874–877 (2014).
16. Zhou, J. *et al*. Co_3O_4-cored carbon dots for chemiluminescence analysis of intracellular hydrogen peroxide. *RSC Advances* **6**, 39480–39483 (2016).
17. Wei, J. *et al*. Fluorescence turn-off detection of hydrogen peroxide and glucose directly using carbon nanodots as probes. *Analytical Methods* **6**, 1922–1927 (2014).
18. Zhao, Q. *et al*. Colorimetric and ultra-sensitive fluorescence resonance energy transfer determination of H_2O_2 and glucose by multi-functional Au nanoclusters. *Analyst* **139**, 1498–1503 (2014).
19. Yang, L. *et al*. Fluorescent Nanocomposite for Visualizing Cross-Talk between MicroRNA-21 and Hydrogen Peroxide in Ischemia-Reperfusion Injury in Live Cells and *In Vivo*. *Analytical Chemistry* **88**, 11886–11891 (2016).
20. Qiao, J., Liu, Z., Tian, Y., Wu, M. & Niu, Z. Multifunctional self-assembled polymeric nanoprobes for FRET-based ratiometric detection of mitochondrial H_2O_2 in living cells. *Chemical Communications* **51**, 3641–3644 (2015).
21. Tao, Y., Ju, E., Ren, J. & Qu, X. Polypyrrole nanoparticles as promising enzyme mimics for sensitive hydrogen peroxide detection. *Chemical Communications* **50**, 3030–3032 (2014).
22. Huang, X., Lan, T., Zhang, B. & Ren, J. Gold nanoparticle–enzyme conjugates based FRET for highly sensitive determination of hydrogen peroxide, glucose and uric acid using tyramide reaction. *Analyst* **137**, 3659–3666 (2012).
23. Zhang, Q. & Kong, D.-M. A general fluorescent sensor design strategy for "turn-on" activity detection of exonucleases and restriction endonucleases based on graphene oxide. *Analyst* **138**, 6437–6444 (2013).
24. Liu, J., Liu, G., Liu, W. & Wang, Y. Turn-on fluorescence sensor for the detection of heparin based on rhodamine B-modified polyethyleneimine–graphene oxide complex. *Biosensors and Bioelectronics* **64**, 300–305 (2015).
25. Lu, L. *et al*. Detection of nicking endonuclease activity using a G-quadruplex-selective luminescent switch-on probe. *Chemical Science* **5**, 4561–4568 (2014).
26. Wang, M., Wang, W., Kang, T.-S., Leung, C.-H. & Ma, D.-L. Development of an Iridium (III) complex as a G-quadruplex probe and its application for the G-quadruplex-based luminescent detection of picomolar insulin. *Analytical chemistry* **88**, 981–987 (2015).
27. Leung, K.-H. *et al*. Label-free luminescence switch-on detection of hepatitis C virus NS3 helicase activity using a G-quadruplex-selective probe. *Chemical Science* **6**, 2166–2171 (2015).
28. Bhattacharjee, Y. & Chakraborty, A. Label-free cysteamine-capped silver nanoparticle-based colorimetric assay for Hg (II) detection in water with subnanomolar exactitude. *ACS Sustainable Chemistry & Engineering* **2**, 2149–2154 (2014).
29. Liu, F., Bing, T., Shangguan, D., Zhao, M. & Shao, N. Ratiometric Fluorescent Biosensing of Hydrogen Peroxide and Hydroxyl Radical in Living Cells with Lysozyme–Silver Nanoclusters: Lysozyme as Stabilizing Ligand and Fluorescence Signal Unit. *Analytical Chemistry* **88**, 10631–10638 (2016).
30. Zhu, D. *et al*. Coordination-Mediated Programmable Assembly of Unmodified Oligonucleotides on Plasmonic Silver Nanoparticles. *ACS applied materials & interfaces* **7**, 11047–11052 (2015).
31. Chen, S., Hai, X., Chen, X.-W. & Wang, J.-H. *In situ* growth of silver nanoparticles on graphene quantum dots for ultrasensitive colorimetric detection of H_2O_2 and glucose. *Analytical chemistry* **86**, 6689–6694 (2014).
32. Cao, X., Shen, F., Zhang, M. & Sun, C. Rapid and highly-sensitive melamine sensing based on the efficient inner filter effect of Ag nanoparticles on the fluorescence of eco-friendly ZnSe quantum dots. *Sensors and Actuators B: Chemical* **202**, 1175–1182 (2014).
33. Ran, X., Sun, H., Pu, F., Ren, J. & Qu, X. Ag nanoparticle-decorated graphene quantum dots for label-free, rapid and sensitive detection of Ag^+ and biothiols. *Chemical Communications* **49**, 1079–1081 (2013).
34. Li, Y. *et al*. A homogeneous assay for highly sensitive detection of CaMV35S promoter in transgenic soybean by förster resonance energy transfer between nitrogen-doped graphene quantum dots and Ag nanoparticles. *Analytica Chimica Acta* **948**, 90–97 (2016).
35. Li, J. *et al*. Fluorescence turn-on detection of glucose via the Ag nanoparticle mediated release of a perylene probe. *Chemical Communications* **51**, 6354–6356 (2015).
36. Zhang, Y. *et al*. One-pot green synthesis of Ag nanoparticles-graphene nanocomposites and their applications in SERS, H_2O_2, and glucose sensing. *Rsc Advances* **2**, 538–545 (2012).
37. Han, D.-M., Zhang, Q. M. & Serpe, M. J. Poly (N-isopropylacrylamide)-co-(acrylic acid) microgel/Ag nanoparticle hybrids for the colorimetric sensing of H_2O_2. *Nanoscale* **7**, 2784–2789 (2015).
38. Zhang, Q. *et al*. Dissolving Ag from Au− Ag Alloy Nanoboxes with H_2O_2: A Method for Both Tailoring the Optical Properties and Measuring the H_2O_2 Concentration. *The Journal of Physical Chemistry C* **114**, 6396–6400 (2010).
39. Kumar, A., Vyas, G., Bhatt, M., Bhatt, S. & Paul, P. Silver nanoparticle based highly selective and sensitive solvatochromatic sensor for colorimetric detection of 1, 4-dioxane in aqueous media. *Chemical Communications* **51**, 15936–15939 (2015).
40. Bai, J. & Jiang, X. A facile one-pot synthesis of copper sulfide-decorated reduced graphene oxide composites for enhanced detecting of H_2O_2 in biological environments. *Analytical chemistry* **85**, 8095–8101 (2013).
41. Wu, S., Tan, S. Y., Ang, C. Y., Luo, Z. & Zhao, Y. Oxidation-triggered aggregation of gold nanoparticles for naked-eye detection of hydrogen peroxide. *Chemical Communications* **52**, 3508–3511 (2016).
42. Zhang, Y. *et al*. Highly sensitive graphene–Pt nanocomposites amperometric biosensor and its application in living cell H_2O_2 detection. *Analytical chemistry* **86**, 9459–9465 (2014).
43. Narayanaswamy, N. *et al*. Stimuli-responsive colorimetric and NIR fluorescence combination probe for selective reporting of cellular hydrogen peroxide. *Chemical Science* **7**, 2832–2841 (2016).
44. Lu, W., Luo, Y., Chang, G. & Sun, X. Synthesis of functional SiO_2-coated graphene oxide nanosheets decorated with Ag nanoparticles for H_2O_2 and glucose detection. *Biosensors and Bioelectronics* **26**, 4791–4797 (2011).
45. Wang, G.-L., Zhu, X.-Y., Jiao, H.-J., Dong, Y.-M. & Li, Z.-J. Ultrasensitive and dual functional colorimetric sensors for mercury(II) ions and hydrogen peroxide based on catalytic reduction property of silver nanoparticles. *Biosensors and Bioelectronics* **31**, 337–342 (2012).
46. Zhao, Q. *et al*. A Highly Selective and Multisignaling Optical− Electrochemical Sensor for Hg^{2+} Based on a Phosphorescent Iridium(III) Complex. *Organometallics* **26**, 2077–2081 (2007).
47. Liu, J.-B. *et al*. A long lifetime iridium(III) complex as a sensitive luminescent probe for bisulfite detection in living zebrafish. *Sensors and Actuators B: Chemical* **243**, 971–976 (2017).
48. Ko, C.-N. *et al*. A long-lived phosphorescence iridium(III) complex as a switch on-off-on probe for live zebrafish monitoring of endogenous sulfide generation. *Biosensors and Bioelectronics* **94**, 575–583 (2017).
49. Liu, J.-B. *et al*. An Aldol Reaction-Based Iridium(III) Chemosensor for the Visualization of Proline in Living Cells. *Scientific Reports* **6**(1) (2016).

Acknowledgements

This work is supported by Hong Kong Baptist University (FRG2/15–16/002), the Health and Medical Research Fund (HMRF/14130522, 14150561), the Research Grants Council (HKBU/12301115, HKBU/204612 and HKBU/201913), the National Natural Science Foundation of China (21575121, 21628502), the Guangdong Province Natural Science Foundation (2015A030313816), the Hong Kong Baptist University Century Club Sponsorship Scheme 2016, the Interdisciplinary Research Matching Scheme (RC-IRMS/15–16/03), Innovation and Technology Fund (ITS/260/16FX), Matching Proof of Concept Fund (MPCF-001-2017/18), the Science and Technology Development Fund, Macao SAR (077/2016/A2, 007/2014/AMJ), and the University of Macau (MYRG2015–00137-ICMS-QRCM, MYRG2016–00151-ICMS-QRCM and MRG044/LCH/2015/ICMS).

Author Contributions

Jinshui Liu contributed to the sensing experiments and muniscript draft; Zhen-Zhen Dong prepared the iridium complex, SEM and TEM experiments; Chao Yang and Guodong Li completed the cell imaging and MTT experiments; Chun Wu helped to draw and arrange the Figures 1–5 in the manuscript; Fu-Wa Lee mainly commented and reviesed the manuscript; Chung-Hang Leung and Dik-Lung Ma proposed and instructed the project.

Additional Information

Supplementary information accompanies this paper at doi:10.1038/s41598-017-09478-6

Competing Interests: The authors declare that they have no competing interests.

Publisher's note: Springer Nature remains neutral with regard to jurisdictional claims in published maps and institutional affiliations.